ISSN 1674-1056
http://cpb.iphy.ac.cn
http://iopscience.iop.org/cpb
中国物理 B
Chinese Physics
中国物理 Chinese Physics B

Thermoelectric properties of lower concentration K-doped $Ca_3Co_4O_9$ ceramics

Ya-Nan Li(李亚男), Ping Wu(吴平), Shi-Ping Zhang(张师平), Sen Chen(陈森), Dan Yan(闫丹), Jin-GuangYang(杨金光), Li Wang(王立), Xiu-Lan Huai(淮秀兰)
Citation: Chin. Phys. B . 2018, 27(5): 057201. **doi:** 10.1088/1674-1056/27/5/057201

Journal homepage: http://cpb.iphy.ac.cn; http://iopscience.iop.org/cpb

What follows is a list of articles you may be interested in

Enhanced thermoelectric properties of p-type polycrystalline SnSe by regulating the anisotropic crystal growth and Sn vacancy

Chengyan Liu(刘呈燕), Lei Miao(苗蕾), Xiaoyang Wang(王潇漾), Shaohai Wu(伍少海), Yanyan Zheng(郑岩岩), Ziyang Deng(邓梓阳), Yulian Chen(陈玉莲), Guiwen Wang(王桂文), Xiaoyuan Zhou(周小元)
Chin. Phys. B . 2018, 27(4): 047211. **doi:** 10.1088/1674-1056/27/4/047211

Enhanced thermoelectric performance in p-type Mg_3Sb_2 via lithium doping

Hao Wang(王浩), Jin Chen(陈进), Tianqi Lu(陆天奇), Kunjie Zhu(朱坤杰), Shan Li(李珊), Jun Liu(刘军), Huaizhou Zhao(赵怀周)
Chin. Phys. B . 2018, 27(4): 047212. **doi:** 10.1088/1674-1056/27/4/047212

Biaxial strain-induced enhancement in the thermoelectric performance of monolayer WSe_2

Wanhuizi Shen(沈婉慧子), Daifeng Zou(邹代峰), Guozheng Nie(聂国政), Ying Xu(许英)
Chin. Phys. B . 2017, 26(11): 117202. **doi:** 10.1088/1674-1056/26/11/117202

Thermoelectric properties of Li-doped $Sr_{0.7}Ba_{0.3}Nb_2O_{6-\delta}$ ceramics

Ya-Cui Zhang(张亚翠), Jian Liu(刘剑), Yi Li(李宜), Yu-Fei Chen(陈宇飞), Ji-Chao Li(李吉超), Wen-Bin Su(苏文斌), Yu-Cheng Zhou(周昱成), Jin-Ze Zhai(翟近泽), Teng Wang(王腾), Chun-Lei Wang(王春雷)
Chin. Phys. B . 2017, 26(10): 107201. **doi:** 10.1088/1674-1056/26/10/107201

Optimize the thermoelectric performance of CdO ceramics by doping Zn

Xin-Yu Zha(查欣雨), Lin-Jie Gao(高琳洁), Hong-Chang Bai(白洪昌), Jiang-Long Wang(王江龙), Shu-Fang Wang(王淑芳)
Chin. Phys. B . 2017, 26(10): 107202. **doi:** 10.1088/1674-1056/26/10/107202

Thermoelectric properties of lower concentration K-doped $Ca_3Co_4O_9$ ceramics*

Ya-Nan Li(李亚男)[1], Ping Wu(吴平)[1,†], Shi-Ping Zhang(张师平)[1], Sen Chen(陈森)[1], Dan Yan(闫丹)[1], Jin-GuangYang(杨金光)[1], Li Wang(王立)[2], and Xiu-Lan Huai(淮秀兰)[3]

[1] *Beijing Key Laboratory for Magneto-Photoelectrical Composite and Interface Science, School of Mathematics and Physics, University of Science and Technology Beijing, Beijing* 100083, *China*

[2] *School of Energy and Environmental Engineering, University of Science and Technology Beijing, Beijing* 100083, *China*

[3] *Institute of Engineering Thermophysics, Chinese Academy of Sciences, Beijing* 100190, *China*

(Received 5 February 2018; revised manuscript received 9 March 2018; published online 26 April 2018)

The tuning of electron and phonon by ion doping is an effective method of improving the performances of thermoelectric materials. A series of lower concentration K-doped $Ca_{3-x}K_xCo_4O_9$ ($x = 0$, 0.05, 0.10, 0.15) polycrystalline ceramic samples are prepared by combining citrate acid sol-gel method with cold-pressing sintering method. The single-phase compositions and plate-like grain morphologies of all samples are confirmed by x-ray diffraction and field emission scanning electron microscope. The effects of lower concentration K doping on the thermoelectric properties of the material are evaluated systematically at high temperatures (300–1026 K). Low concentration K doping causes electrical conductivity to increase up to 23% with little effect on the Seebeck coefficient. Simultaneously, the thermal conductivity of K-doped sample is lower than that of the undoped sample, and the total thermal conductivity reaches a minimum value of approximately 1.30 $W{\cdot}m^{-1}{\cdot}K^{-1}$, which may be suppressed mainly by the phonon thermal conduction confinement. The dimensionless figure-of-merit ZT of $Ca_{2.95}K_{0.05}Co_4O_9$ is close to 0.22 at 1026 K, representing an improvement of about 36% compared with that of $Ca_3Co_4O_9$, suggesting that lower concentration K-doped $Ca_3Co_4O_9$ series materials are promising thermoelectric oxides for high-temperature applications.

Keywords: $Ca_3Co_4O_9$, thermoelectric properties, ceramics

PACS: 72.15.Jf, 84.60.Rb, 81.05.Je **DOI:** 10.1088/1674-1056/27/5/057201

1. Introduction

Under the serious situations of resource shortage and environmental pollution, thermoelectric (TE) materials, which can directly convert heat energy to electrical power and vice versa, play a significant role in meeting energy challenges in the future.[1,2] The energy conversion efficiency of a TE material is found to depend on the dimensionless figure-of-merit, ZT which is defined as $ZT = \sigma S^2 T/\kappa$, where σ, S, T, and κ are the electrical conductivity, Seebeck coefficient, absolute temperature, and thermal conductivity, respectively. As can be observed from the formula, a combination of high electrical conductivity and Seebeck coefficient is desired, whereas thermal conductivity must be low for applicable TE materials.[3,4] Over the past few decades, intermetallic compounds, such as Bi_2Te_3 and SnSe, have been widely investigated because of their superior thermal performances,[5,6] but oxide TE materials, such as $NaCo_2O_4$, $Ca_3Co_4O_9$, and $CaMnO_3$, have attracted the attention of scientific workers in recent years due to their high thermal and chemical stabilities, lower cost, and non-rare or non-toxic elements.[7–9] Among these transition metal oxides, $Ca_3Co_4O_9$ is considered to be a promising oxide TE material on account of its high electrical conductivity, low thermal conductivity, and high thermostability at approximately 1000 K in the air.[10] The $Ca_3Co_4O_9$, with misfit-layered structure, is composed of NaCl-type Ca_2CoO_3 and CdI2-type CoO_2 layers.[11] The Ca_2CoO_3 layer is commonly considered to be responsible for charge reservoir and structure stabilizer. Meanwhile, the charge carriers mainly transport in the CoO_2 layer. These two sublattices possess the same a- and c-axis lattice parameters and β angles but different b-axis lengths, leading to a misfit along the b-direction. These strong electron correlated systems with misfit layer structures are subject to a crucial condition for the highly thermoelectric performance of $Ca_3Co_4O_9$.[11,12] The ZT of single-crystalline $Ca_3Co_4O_9$ can reach 0.87 at around 973 K.[13] Unfortunately, the ZT of polycrystalline $Ca_3Co_4O_9$ is relatively low for practical use; thus, numerous studies have shown that the carrier conduction in polycrystalline $Ca_3Co_4O_9$ TE material can be controlled by doping other elements into the system at the Ca[14–16] or Co[17–19] sites to improve the TE properties. However, these studies mainly use rare-earth metals, alkaline-earth metals, or toxic elements of doping to improve the performance of $Ca_3Co_4O_9$ at present.[15,20,21] The K element as an environmentally friendly element was generally selected as p-type dopant for tuning the carrier concentration

*Project supported by the National Key R&D Program of China (Grant No. 2016YFB0601101) and the National Natural Science Foundation of China (Grant No. 51476173).

†Corresponding author. E-mail: pingwu@sas.ustb.edu.cn

© 2018 Chinese Physical Society and IOP Publishing Ltd

and microstructure, indicating its potential for achieving a high ZT.[22,23] Based on the theoretical analysis, the substitution of monovalent K^+ for divalent Ca^{2+} of the $Ca_3Co_4O_9$ may increase the carrier concentration. The K and Ca elements have similar atomic mass values, but the radius of the K ion (1.33 Å) is larger than that of the Ca ion (1.00 Å), which may cause lattice to deform, phonon scattering to be enhanced, and the material TE properties to improve. To our knowledge, Lim *et al.*[24] have studied the effects of higher concentration K-doping on $Ca_{3-x}K_xCo_4O_9$ (x = 0, 0.1, 0.2, 0.3), in which the conductivity of K-doped sample was found to be higher than that of undoped sample, but the most of the thermal conductivities were higher than that of the undoped sample. However, it can be seen from the results of the study that when the doping concentration was low (x = 0.1), the thermal conductivity was lower than that of the undoped sample in a temperature range of about 700–1100 K. It can be hypothesized that the lower concentration doping will be more conducive to reduce the thermal conductivity. Lan *et al.*[25] studied the TE properties of $Bi_{1-x}K_xCuSeO$ ($0 \leq x \leq 0.10$). When the K content was x = 0.02, the ZT was increased by 50% at 823 K compared with the undoped sample. When the doping concentration is larger, the increase is smaller or even lower than that of the original sample. Similarly, Zhang *et al.*[26] found that the thermal conductivities of the lower concentration of Ag-doped $Ca_{3-x}Ag_xCo_4O_{9+\delta}$ (x = 0, 0.01, 0.03, 0.05) were lower than that of the undoped sample, and when the doping content x = 0.01, the conductivity was the highest, and the conductivity decreases with the increase in the doping content. Therefore, it is necessary to investigate the effect of lower concentration K doping on the TE performance of $Ca_3Co_4O_9$.

In this work, polycrystalline $Ca_{3-x}K_xCo_4O_9$ (x = 0, 0.05, 0.10, 0.15) ceramic samples (where the x value is the apparent concentration of K element) are prepared by the combined methods of sol-gel and cold-pressing. The TE properties of the lower concentration K doping polycrystalline $Ca_{3-x}K_xCo_4O_9$ (x = 0, 0.05, 0.10, 0.15) ceramic materials are investigated systematically, and a method of improving the TE properties of cobalt oxides is explored.

2. Experiment

The $Ca_{3-x}K_xCo_4O_9$ (x = 0, 0.05, 0.10, 0.15) precursor powders were synthesized by citrate acid sol-gel method. Stoichiometric ratios of $Ca(NO_3)_2{\cdot}4H_2O$, $Co(NO_3)_2{\cdot}6H_2O$, and $KNO_3{\cdot}H_2O$ were dissolved thoroughly in deionized water, and a certain amount of citric acid was added. The solution was heated under continuous stirring at 353 K in the air until the gel was formed. The gel was dried at 393 K in the air for 8 h. Then, the dry gel was ground, combusted at 572 K in the air, and calcined at 1073 K for 8 h in the air to produce the $Ca_{3-x}K_xCo_4O_9$ powder. Finally, the powder was reground and pressed at 30 MPa to form pellets, which were sintered at 1073 K for 8 h in the air. The phase compositions of all bulk specimens were analyzed using x-ray diffraction (XRD) with a RigakuD/max-2500 diffractometer equipped with Cu Kα radiation at room temperature in the air. The diffraction intensities were collected in the 2θ range from 5° to 65° in steps of 0.01°. The microstructure was observed with the field emission scanning electron microscope (FESEM, Zeiss Supra 55). Electrical conductivity and Seebeck coefficient were simultaneously conducted in Ar atmosphere from room temperature up to 1026 K on Seebeck Coefficient/Electric Conductivity Measuring System (Netzsch SBA458). The thermal conductivity was calculated by $k = DC_pd$, and the density d was determined by the geometric density. The specific heat capacity C_p was determined by differential scanning calorimeter (Netzsch DSC/STA409PC), and the thermal diffusivity coefficient D was measured by the laser-flash method (Netzsch Instruments/LAF457).

3. Results and discussion

3.1. Structure and composition analysis

Figure 1(a) shows the XRD patterns of the sintered $Ca_{3-x}K_xCo_4O_9$ (x = 0, 0.05, 0.10, 0.15) bulk materials in the direction perpendicular to pressure direction, and the diffraction peaks are marked. All the diffraction peaks can be indexed as $Ca_3Co_4O_9$ structure according to the JCPDS card with PDF No.21-0110, and no secondary phase was found, indicating that the prepared bulk materials are $Ca_3Co_4O_9$ compounds, and the K has successfully entered into the lattice site.[18,27] As shown in Fig. 1(a), the diffraction peaks of (00l) planes are much stronger than other peaks. The orientation factor L is calculated by using XRD pattern to further analyze the grain orientation of the bulk sample. L can be expressed as $L = (P - P_0)/(1 - P_0)$, where $P = \Sigma I\{00l\}/\Sigma I\{hkl\}$, with I being the intensity of the diffraction peak, and P values are calculated from the XRD patterns of doped $Ca_{3-x}K_xCo_4O_9$ (x = 0, 0.05, 0.10, 0.15) samples; P_0 is calculated from randomly grain oriented sample by using standard PDF card JCPDS (No.21-0110). The value of L is equal to 1 when the pressure direction is oriented along the crystal c-axis completely. Figure 1(b) shows the relationship between the L and the doping content of K. The L of all the samples were around 0.85, indicating that these ceramic samples in the c-direction have an obviously preferred orientation by the cold-pressure method, that is, the grains preferred to grow in the direction perpendicular to the pressure. The density of $Ca_{3-x}K_xCo_4O_9$ (x = 0, 0.05, 0.10, 0.15) samples is approximately 81% of the theoretical value (4.94 g/cm^3)[11] as shown in Fig. 1(c). Studies have shown that spark plasma sintering (SPS) technique[28,29] and hot press (HP) technique[28] each can make the sample

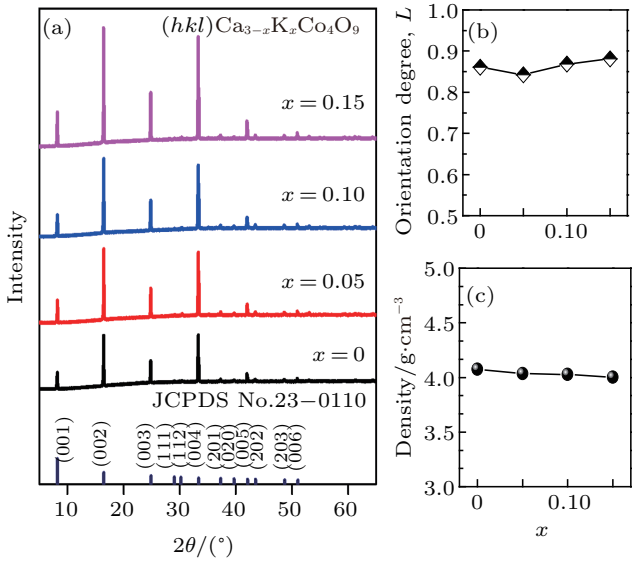


Fig. 1. (color online) (a) XRD patterns of sintered $Ca_{3-x}K_xCo_4O_9$ ($x = 0$, 0.05, 0.10, 0.15) bulk samples in the direction perpendicular to pressure direction, and (b) grain orientation degree (L) and (c) density versus x value of the $Ca_{3-x}K_xCo_4O_9$ samples.

have a higher density. Figure 2 displays the SEM images of $Ca_{3-x}K_xCo_4O_9$ ($x = 0$, 0.05, 0.10, 0.15) bulk samples. Most of the particles with a grain size of several microns are flake-like. Particle size distributions (Fig. 3) of the samples were determined by the software of Nano Measurer program[30] based on the corresponding SEM images. The analyses of a number of the particle show that these samples have average sizes of 0.99 μm, 1.29 μm, 1.41 μm, and 1.64 μm, respectively. With increasing doping content, the sizes of the particles increase.

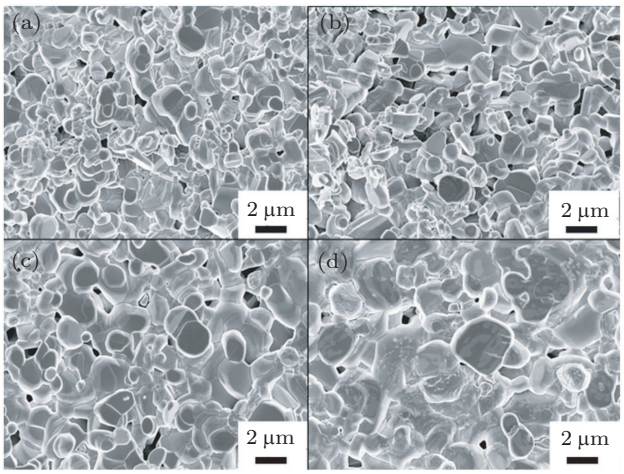


Fig. 2. SEM images of sintered sample surfaces (a) $Ca_3Co_4O_9$, (b) $Ca_{2.95}K_{0.05}Co_4O_9$, (c) $Ca_{2.90}K_{0.10}Co_4O_9$, and (d) $Ca_{2.85}K_{0.15}Co_4O_9$.

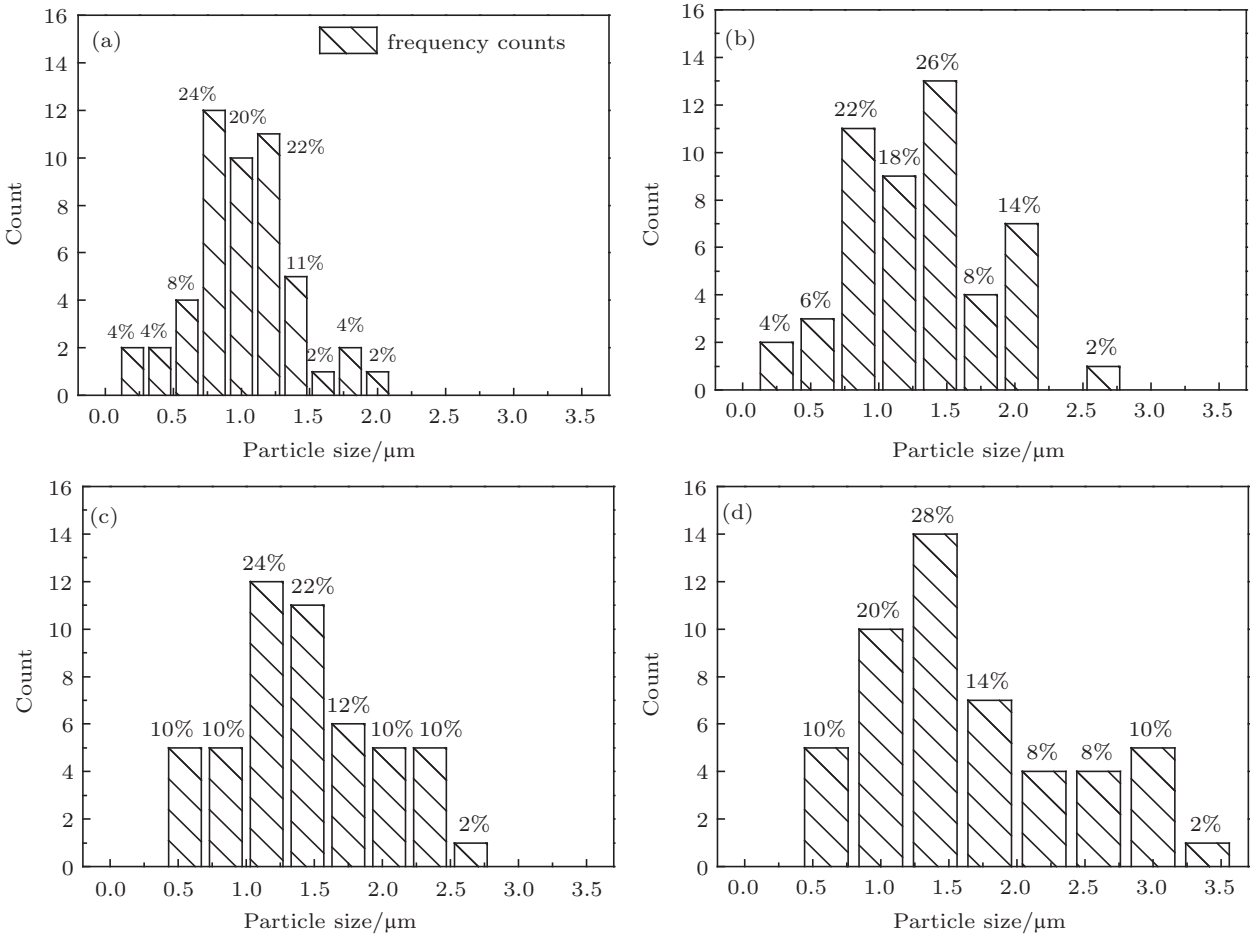


Fig. 3. Particle size distributions of (a) $Ca_3Co_4O_9$, (b) $Ca_{2.95}K_{0.05}Co_4O_9$, (c) $Ca_{2.90}K_{0.10}Co_4O_9$, and (d) $Ca_{2.85}K_{0.15}Co_4O_9$, obtained from the SEM images of 50 particles.

3.2. Electrical transport properties

The relationships between the electrical conductivity and the temperature of the $Ca_{3-x}K_xCo_4O_9$ (x = 0, 0.05, 0.10, 0.15) samples are shown in Fig. 4(a). According to the electrical conductivity formula $\sigma = ne\mu$, where n is the carrier concentration, e is the electron charge of the carrier, and μ is the carrier mobility, the electrical conductivity mainly depends on the carrier concentration and mobility of the sample. Figure 4(a) shows that all electrical conductivity values increase with increasing temperature, which exhibits remarkable semiconductor-like behavior in a temperature range from 400 K to 1026 K. At the same time, it can be seen that when the doping concentration is $x = 0.05$, the conductivity is higher than that of the undoped sample, but with the doping content increasing (x = 0.10, 0.15), the conductivity decreases and becomes lower than that of the undoped sample. In general, when K^+ is substituted for Ca^{2+}, the valence of K is lower than that of Ca, thereby increasing the carrier concentration in the sample. Simultaneously, K doping can form impurity energy level in the semiconductor band gap, reducing the band gap width. This result is conducive for impurity and intrinsic carriers transiting from the valence band to the conduction band to further increase the carrier concentration at room temperature, which leads to the higher electrical conductivity of the doped sample. These can explain why the electrical conductivity of $x = 0.05$ sample is higher than those of the undoped samples. However, the electrical conductivity decreases with the further increase of K doping content. It indicates that the carrier concentration increases and the carrier mobility decreases with the increase of K doping content. Moreover, the effect of carrier concentration on the electrical conductivity is weak compared with that of carrier mobility. Similarly, Pei *et al.*[21] found that the electrical conductivity decreases with the increase of Er-doping for $Ca_{3-x}Er_xCo_4O_{9+\delta}$ ($x = 0.15$, 0.30 and 0.50).

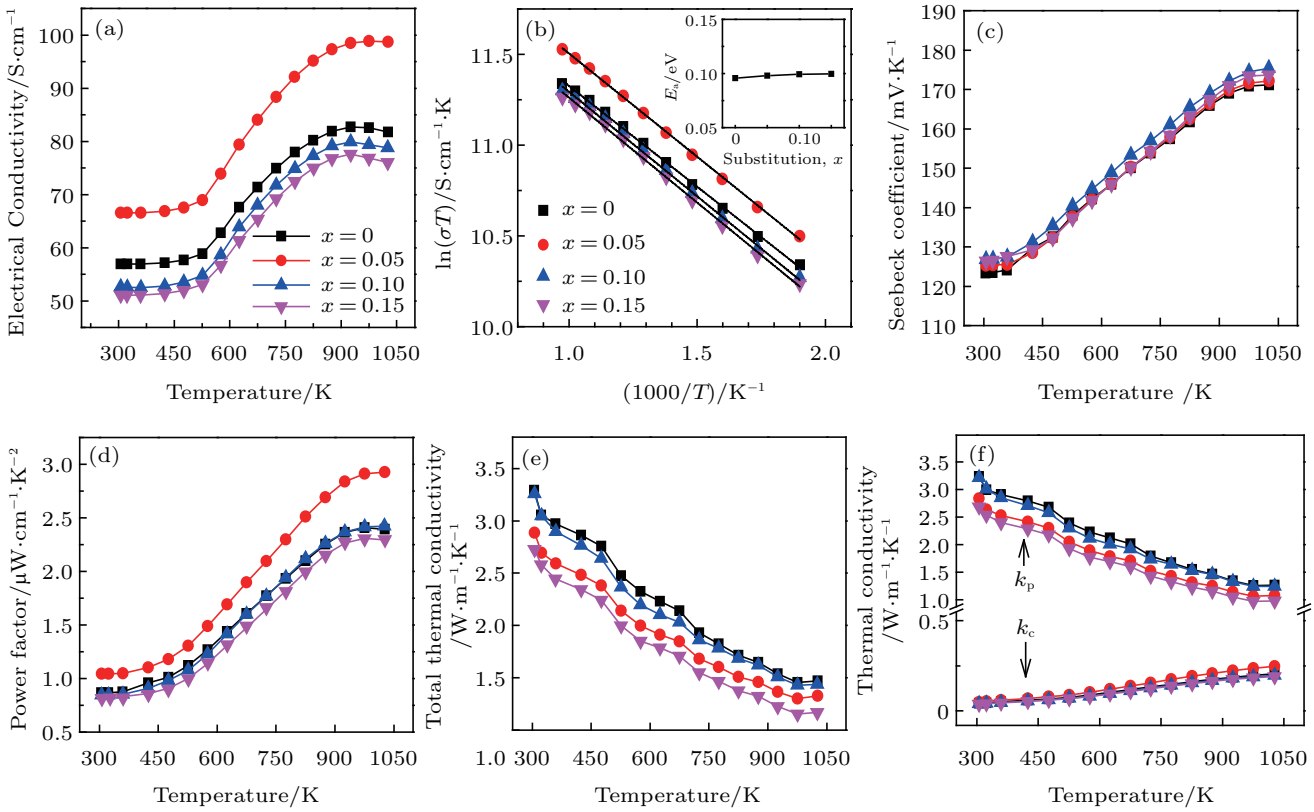


Fig. 4. (color online) Thermoelectric properties of $Ca_{3-x}K_xCo_4O_9$ samples. (a) Temperature-dependent electrical conductivities for $Ca_{3-x}K_xCo_4O_9$ samples. (b) Relationships between $\ln(\sigma T)$ and $1000/T$ for $Ca_{3-x}K_xCo_4O_9$ samples. Inset: K content dependent activation energy (E_a) values. (c) Temperature-dependent Seebeck coefficients. (d) Temperature-dependent power factors. (e) Temperature-dependent total thermal conductivity k values. (f) Temperature-dependent carrier thermal conductivity k_c values and the phonon thermal conductivity k_p values for $Ca_{3-x}K_xCo_4O_9$ samples.

The experimental results can be further explained by the model of electrical conductivity versus temperature. Hopping conduction behavior exists in $Ca_3Co_4O_9$ at high temperature. The electrical conductivity is generally described as $\sigma(T) = \left(Anea^2/T\right)\exp\left(-E_a/k_BT\right)$, where A, E_a, k_B, and a are the pre-exponential terms relating to the scattering mechanism, activation energy, Boltzmann constant, and intersite distance of hopping, respectively.[31] Figure 4(b) shows the linear relationship between $\ln(\sigma T)$ and $1000/T$ in the temperature range above 600 K, indicating that the sample satisfies the conduction mechanism of the hopping conduction behavior. According to the above equation, the value of E_a can be

obtained by linearly fitting the slope. The results are provided in the illustration (R^2 reaches 0.99). The value of E_a hardly changes with the increase of doping concentration. If the K is substituted for the Co ions in the CoO_2 layer, the defect would be brought into the conduction path, and thus may have a significant effect on the activation energy. However, if the substitution is in the Ca_2CoO_3 layer, the conduction path will not be disturbed and will have little effect on the activation energy. Thus, K ions should be substituted for the Ca sites in the crystal lattice.[18,32,33] Although further research is generally necessary, lower concentration K doping favors the increase of the electrical conductivity of $Ca_3Co_4O_9$ ceramic oxide. The electrical conductivity of $Ca_{2.95}K_{0.05}Co_4O_9$ sample is approximately 23% higher than that of the undoped $Ca_3Co_4O_9$ sample, and lower concentration K doping has a significant effect on improving the $Ca_3Co_4O_9$ electric properties.

The temperature-dependent Seebeck coefficient S values of all the samples are shown in Fig. 4(c). The sign of S is positive for the entire measured temperature range, confirming a dominant p-type conduction mechanism. The Seebeck coefficients of all the samples increase with increasing temperature. This result may be related to the phonon traction effect, that is, the phonon flows from the high-temperature end of the semiconductor to the low-temperature side, transfers energy to the carrier by collision, and then forms the seam stream with the phonons, and thus increasing the Seebeck coefficient. Notably, the increase in electrical conductivity is generally accompanied by a decrease in the Seebeck coefficient; however, the Seebeck coefficients of the K-doped and the undoped samples are nearly equal. The $Ca_3Co_4O_9$ is a strong electron correlation system[11] whose Seebeck coefficient can be analyzed according to Heikes expansion formula.[34] The S of the cobalt oxide system can be expressed as

$$S = -\left(\frac{k_B}{e}\right)\ln\left[\frac{d_3 x}{d_4(1-x)}\right], \tag{1}$$

where d_3 and d_4 are the numbers of configurations of the Co^{3+} and Co^{4+} ions, respectively, and x is the concentration of Co^{4+} ions in the CoO_2 layer, with the low spin states of Co^{3+} and Co^{4+} yielding $d_3 = 1$ and $d_4 = 6$. According to the above equation, the value of S increases with decreasing x value, that is, it is assumed that the K ion fraction replaces Co^{4+} in CoO_2, which can reduce the concentration of Co^{4+} ions. Simultaneously, the transition of Co^{4+} state to the low spin state Co^{3+} also reduces x, thereby increasing S. However, S does not change with K doping in the present study, and thus K ions do not enter into the CoO_2 conductive layer,[35] which is consistent with previous E_a analysis. Furthermore, the test results can also be analyzed based on Mott formula[36]

$$S = \frac{C_e}{n} + \frac{\pi^2 k_B^2 T}{3e}\left[\frac{\partial \ln \mu(\varepsilon)}{\partial \varepsilon}\right]_{\varepsilon=E_F}, \tag{2}$$

where c_e, k_B, and $\mu(\varepsilon)$ are the electronic specific heat, Boltzmann constant, and energy correlated carrier mobility, respectively. From the above equation, S mainly depends on the n and $\mu(\varepsilon)$ at a certain temperature. The number of K^+ ions increases the carrier concentration n in the alternative Ca^{2+} based on previous analysis, and the first term of Eq. (2) shows that S decreases as the carrier concentration n increases. However, the results of the present study show that different concentrations of K doping have little effect on the S value of the sample. When K^+ replaces the Ca^{2+} position in the lattice, the energy band structure and the Fermi level E_F of the system will change, and the $\mu(\varepsilon)$ of the second term of the formula may also change. Although dopant increases the carrier concentration, S also increases,[37,38] indicating that $\mu(\varepsilon)$ may have a critical effect on S in this layered cobalt oxide. This result indicates that when the carrier concentration increases, S is almost invariant.

The values of power factor $PF(PF = \sigma S^2)$ of the $Ca_{3-x}K_xCo_4O_9$ (x = 0, 0.05, 0.10, 0.15) series of samples are shown in Fig. 4(d) to estimate the TE properties of the material. As can be observed from the figure, PF increases with increasing temperature, and K doping can regulate the power factor of the sample. For the $Ca_{2.95}K_{0.05}Co_4O_9$ sample, the PF reaches 2.93 $\mu W \cdot cm^{-1} \cdot K^{-2}$ at 1026 K, which is approximately 22% higher than that of the undoped $Ca_3Co_4O_9$ sample. The high PF indicates a relatively high TE conversion power.[39] This result indicates that K doping is an effective method of improving the electrical properties of $Ca_3Co_4O_9$ materials.

3.3. Thermal transport properties

Figure 4(e) shows the relationships between the total thermal conductivity (k) of the sample in the direction perpendicular to the pressure direction and temperature. For all samples, k decreases with increasing temperature. The value of k for the sample doped with K is less than that of the undoped sample. For the $Ca_3Co_4O_9$ system, the k can be represented by the sum of carrier thermal conductivity (k_c) and the phonon thermal conductivity (k_p), i.e., $k = k_c + k_p$, where the carrier thermal conductivity is defined as $k_c = LT\sigma (L = \pi^2 k_B 2/3e^2 = 2.45 \times 10^{-8}\ V^2 \cdot K^{-2})$ according to the Wiedemann–Franz law. The value of k_c is small (Fig. 4(f)); it is approximately only 10% of the total thermal conductivity. Accordingly, k depends mainly on k_p. In the low-order approximation, the phonon thermal conductivity can be given by using the relationship $k_p = cvl_p/3$, where c, v, and l_p represent the specific heat capacity of the phonon, the phonon propagation velocity, and the mean free path, respectively. Typically, such doping will increase c but reduce v and l_p.[40,41] Moreover, the phonon propagation velocity and the mean free path of the phonon are positively correlated.[42] Based on the above analysis, the phonon

thermal conductivity is suppressed, which can be attributed to lattice defects caused by the doping of K and thus causing lattice deformation, thereby enhancing phonon scattering and reducing the average free path of the phonon and the propagation velocity. According to Matthiessen's law, the phonon thermal conductivity mainly depends on the point defect scattering, grain boundary scattering, and the non-harmonic three-phonon Umklapp process (U process) scattering. As a new scattering center, point defect (such as Ca or O vacancies) can further lead to enhanced phonon scattering. Furthermore, the difference between Ca and K ions introduces the spread of stress field, which makes the point defects of the phonon increase and the phonon thermal conductivity decrease. However, there is no regular change in thermal conductivity with the increase of K doping content, which requires further study. However, the lower concentration K doping can be more effective than the higher[24] to reduce the thermal conductivity of the $Ca_3Co_4O_9$.

3.4. Dimensionless thermoelectric figure of merit *ZT*

Figure 5 shows the relationships between the *ZT* of $Ca_{3-x}K_xCo_4O_9$ ($x = 0$, 0.05, 0.10, 0.15) samples and the temperature. The *ZT* values of all samples increase with increasing temperature, which might be attributed mainly to the increase of *S* as the temperature increases and the thermal conductivity decreases. The values of *ZT* of the K-doped samples are higher than those of the undoped *ZT* to a large extent. The value of *ZT* of the $Ca_{2.95}K_{0.05}Co_4O_9$ sample reaches 0.22 at 1026 K, which is an increase of approximately 35% of the undoped $Ca_3Co_4O_9$. The results also show that the TE properties of $Ca_3Co_4O_9$ can be improved by appropriate K doping.

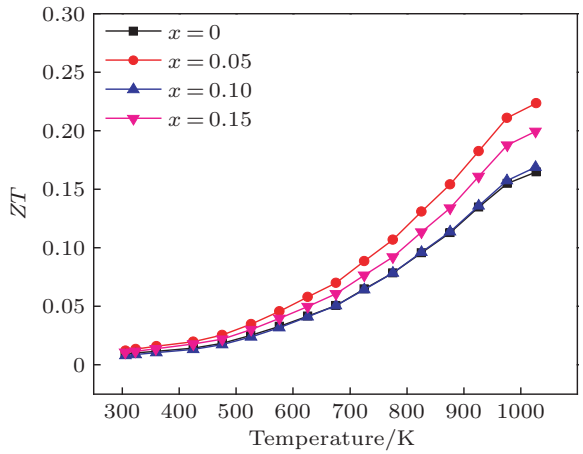


Fig. 5. (color online) Temperature dependent dimensionless figure-of-merit ZT for $Ca_{3-x}K_xCo_4O_9$ ($x = 0$, 0.05, 0.10, 0.15) samples.

4. Conclusions

The TE conductivities of K-doped $Ca_{3-x}K_xCo_4O_9$ ($x = 0$, 0.05, 0.10, 0.15) oxide samples prepared by sol-gel method have been systematically investigated. The XRD and SEM studies show that $Ca_{3-x}K_xCo_4O_9$ samples with $x = 0$, 0.05, 0.10, 0.15 are all of single-phase, and all exhibit similar flake-like morphological structures. An appropriate quantity of K ions doping at the Ca site can effectively increase the electrical conductivity and reduce thermal conductivity of the material.

In all the samples, the power factor of K-doped $Ca_{2.95}K_{0.05}Co_4O_9$ sample reaches 2.93 $\mu W \cdot cm^{-1} \cdot K^{-2}$ at 1026 K and is approximately 22% higher than that of the undoped sample. The value of *ZT* of the $Ca_{2.95}K_{0.05}Co_4O_9$ sample reaches 0.22 at 1026 K and is approximately 35% higher than that of the undoped sample. These results indicate that lower concentration doping is can be used to improve the TE properties of $Ca_3Co_4O_9$ ceramic samples.

References

[1] Disalvo F J 1999 *Science* **285** 703
[2] Biswas K, He J, Blum I D, Chun I, Hogan T P, Seidman D N, Dravid V P and Kanatzidis M G 2012 *Nature* **489** 414
[3] Slack G A and Hussain M A 1991 *J. Appl. Phys.* **70** 2694
[4] Vining C B 1991 *J. Appl. Phys.* **69** 331
[5] Feng S K, Li S M and Fu H Z 2014 *Chin. Phys. B* **23** 117202
[6] Zhao L D, Lo S H, Zhang Y S, Sun H, Tan G J and Uher C 2014 *Nature 508* 373
[7] Terasaki I, Sasago Y and Uchinokura K 1997 *Phys. Rev. B* **56** R12685
[8] Park K and Lee G W 2013 *Energy* **60** 87
[9] Kumar P, Kashyap S C, Sharma V K and Gupta H C 2015 *Chin. Phys. B* **24** 098101
[10] Ohta H, Sugiura K and Koumoto K 2008 *Inorg. Chem.* **47** 8429
[11] Masset A C, Michel C, Maignan A, Hervieu M, Toulemonde O, Studer F, Raveau B and Hejtmanek J 2000 *Phys. Rev. B* **62** 166
[12] Limelette P, Hardy V, Auban-Senzier P, Jérome D, Flahaut D, Hébert S, Frésard R, Simon C h, Noudem J and Maignan A 2005 *Phys. Rev. B* **71** 233108
[13] Shikano M and Funahashi R 2003 *Appl. Phys. Lett.* **82** 1851
[14] Zhang D W, Wang Z H, Tang G D, Xu X B, Xu X N, Qiu L, Zhang D X and Du Y W 2013 *J. Appl. Phys.* **113** 17E113
[15] Xu J, Wei C P and Jia K 2010 *J. Alloy Compd.* **500** 227
[16] Bhaskar A, Lin Z R and Liu C J 2014 *J. Mater. Sci.* **49** 1359
[17] Wang Y, Sui Y, Wang X J, Su W H and Liu X Y 2010 *J. Appl. Phys.* **107** 033708
[18] Prasoetsopha N, Pinitsoontorn S, Kamwanna T, Amornkitbamrung V, Kurosaki K, Ohishi Y, Muta H and Yamanaka S 2014 *J. Alloy Compd.* **588** 199
[19] Torres M A, Rasekh Sh, Constantinescu G, Sotelo A, Bosque P, Madre M A and Diez J C 2015 *J. Mater. Sci. Mater. Electron.* **26** 815
[20] Prevel M, Perez O and Noudem J G 2007 *Solid State Sci.* **9** 231
[21] Pei J, Chen G, Zhou N, Lu D Q and Xiao F 2011 *Physica B* **406** 571
[22] Lee D S, An T H, Jeong M, Choi H S, Lim Y S, Seo W S, Park C H, Park C and Park H H 2013 *Appl. Phys. Lett.* **103** 232110
[23] Wu H J, Zhao L D, Zheng F S, Wu D, Pei Y L and Tong X 2014 *Nat.Commun.* **5** 4515
[24] Lim C H, Choi S M and Seo W S 2010 *J. Korean Phys. Soc.* **57** 1054
[25] Lan J L, Ma W Q, Deng C J, Ren G K, LinY H and Yang X P 2007 *J. Mater. Sci.* **52** 11569
[26] Zhang F P, Zhang X, Lu Q M, Zhang J X, Liu Y Q and Zhang G Z 2011 *Solid State Ion.* **20** 1
[27] Tian Z Y, Wang X H, Liu J, Lin Z J, Hu Y S, Wu Y G, Han C and Hu Z Y 2016 *J. Alloy Compd.* **661** 161
[28] Matsubara I, Funahashi R, Takeuchi T and Sodeoka S 2001 *J. Appl. Phys.* **90** 462
[29] Liu Y, Lin Y, Shi Z, Nan C W and Shen Z J 2005 *J. Am. Ceram. Soc.* **88** 1337
[30] Shi Y R, Wang Y H, Wang D, Liu B, Li Y H and Wei L 2012 *Cryst. Growth Des.* **12** 1785
[31] Bosman A J and Van Daal H J 1970 *Adv. Phys.* **9** 1
[32] Zhang F P, Zhang X, Lu Q M, Zhang J X, Liu Y Q and Zhang G Z 2011 *Solid State Sci.* **13** 1443

[33] Huang C S, Zhang F P, Zhang X, Lu Q M, Zhang J X and Liu Z Y 2016 *J. Alloy Compd.* **6** 87
[34] Koshibae W, Tsutsui K and Maekawa S 2000 *Phys. Rev. B* **62** 6869
[35] Constantinescu G, Rasekh Sh, TorresMA, Bosquec P, Diez J C, Madre M A and Sotelo A 2015 *Ceram. Int.* **41** 10897
[36] Zhao B C, Sun Y P, Lu W J, Zhu X B and Song W H 2006 *Phys. Rev. B* **74** 144417
[37] Bhaskar A, Lin Z R and Liu C J 2013 *J. Mater. Sci.* **49** 1359
[38] Xu G J, Funahashi R, Shikano M, Pu Q R and Liu B 2002 *Solid State Commun.* **124** 73
[39] Narducci D 2011 *Appl. Phys. Lett.* **99** 102104
[40] Takahata K, Iguchi Y, Tanaka D and Itoh T 2000 *Phys. Rev. B* **61** 12551
[41] Zhang F P, Zhang X, Lu Q M, Zhang J X and Liu Y Q 2011 *J. Alloy Compd.* **509** 4171
[42] Li J C, Wang C L, Wang M X, Peng H, Zhang R Z, Zhao M L, Liu J, Zhang J L and Mei L M 2009 *J. Appl. Phys.* **105** 043503